Photocatalytic degradation of methyl orange by nano-TiO_2 thin films prepared by RF magnetron sputtering

Fanming Meng (孟凡明)[1,2,3*], Ling Cao (曹 铃)[1,3], Xueping Song (宋学萍)[1,3], and Zhaoqi Sun (孙兆奇)[1,3]

[1] *School of Physics and Materials Science, Anhui University, Hefei 230039, China*

[2] *State Key Laboratory of Materials Modification by Laser, Ion and Electron Beams, Dalian University of Technology, Dalian 116024, China*

[3] *Anhui Key Laboratory of Information Materials and Devices, Anhui University, Hefei 230039, China*

[*] *E-mail: mrmeng@ahu.edu.cn*

Received December 31, 2008

Nano-TiO_2 thin films are deposited by radio frequency (RF) magnetron sputtering using TiO_2 ceramic target and characterized by X-ray diffractometer, atomic force microscope, and ultraviolet-visible spectrophotometer. The photocatalytic activity is evaluated by light-induced degradation of methyl orange solutions (5, 10, and 20 ppm) using a high pressure mercury lamp as the light source. The film is amorphous, and its energy gap is 3.02 eV. The photocatalytic degradation of methyl orange solution is the first-order reaction and the apparent reaction rate constants are 0.00369, 0.0024, and 0.00151 for the methyl orange solution concentrations of 5, 10, and 20 ppm, respectively.

OCIS codes: 240.6670, 310.6860.

doi: 10.3788/COL20090710.0956.

In 1972, Fujishima *et al.* discovered the photocatalytic splitting of water on TiO_2 electrodes[1]. This event marked the beginning of a new era in heterogeneous photocatalysis. Recently, heterogeneous photocatalysis has attracted growing attention in which TiO_2 thin films is used as an advanced water treatment and water purification process. TiO_2 thin films can be prepared by numerous techniques such as chemical vapor deposition[2], electron beam evaporation[3], ion assisted deposition[4,5], sol-gel processes[6,7], and sputtering[8]. Among these techniques, radio frequency (RF) magnetron sputtering[9] provides more advantages in controlling the microstructure and compositions of the films. In this letter, TiO_2 thin films are deposited on silicon and glass substrates by RF magnetron sputtering. The characteristics including phase structure, surface topography, energy gap, and photocatalytic activity of the films are studied.

TiO_2 thin films were deposited by a high vacuum multifunctional magnetron sputtering equipment (JGP560I) using TiO_2 ceramic targets (Φ=60 mm) on silicon (10×10 mm^2) and glass (43×26 mm^2) substrates at room temperature. Prior to deposition, the substrates were ultrasonically cleaned with acetone, absolute ethyl alcohol, and de-ionized water for 10 min, respectively. When the sputtering chamber was evacuated to 8×10^{-4} Pa, argon gas was introduced. Before the films were deposited, TiO_2 ceramic target was pre-sputtered by argon ions for 3 min to weed out the surface adsorption. During sputtering, the argon gas flow rate was kept at 30 sccm, the chamber pressure was maintained at 0.8 Pa, sputtering power was 60 W, the distance between the substrate and the target was 60 mm, and the sputtering time was 30 min. The film thickness, measured by a surface profiler meter (Ambios XP-1), was 150 nm. The crystallization behavior of the film was analyzed by an X-ray diffractometer (XRD, MAC M18XHF) using Cu Kα radiation. Surface morphological features were observed by an atomic force microscope (AFM, AJ-IIIa). Transmission spectra were obtained by an ultraviolet-visible (UV-Vis) spectrophotometer (SHIMADZU UV-2550(PC) Series). The photocatalytic activity of the film was characterized by degradation of methyl orange ($C_{14}H_{14}N_3NaO_3S$) solutions with concentrations of 5, 10, and 20 ppm, respectively. Firstly, to find the relation between concentration and absorbance of methyl orange solution, methyl orange solutions of 0, 0.5, 1, 2.5, 5, 10, and 20 ppm were prepared, respectively. The transmittances of the methyl orange solutions were measured by an UV-Vis spectrophotometer (SHIMADZU UV-2550), and then transformed into absorbance, further, the wavelength corresponding to the maximum absorbance could be obtained. The relation between concentration and absorbance of methyl orange solution could be obtained from the wavelength of the maximum absorbance. Secondly, the experiment was performed in a 30-ml glass container. The light source was a 36-W high pressure mercury lamp, which emitted visible light of 404.7, 435.8, 546.1, 577.0–579.0 nm, and ultraviolet (UV) light of 365 nm. One sample of glass substrate was horizontally placed at the bottom of the testing cell containing 10-ml methyl orange solution. The distance between the sample and the high pressure mercury lamp was 3.1 cm. The transmittance of the methyl orange solution was measured at intervals of 20 min and the total irradiation time was 3 h. The degradation rate of methyl orange could be obtained by[10]

$$\eta = (C_0 - C_t)/C_0 \times 100\%, \tag{1}$$

where η is the degradation rate of methyl orange after t-min reaction, C_t is the concentration of methyl orange after t-min reaction, and C_0 is the initial concentration.

Figure 1 shows the XRD patterns of as-deposited TiO_2 thin film and silicon substrate. It can be seen that there is not any characteristic peak of anatase, rutile, and brookite in the XRD pattern of TiO_2 thin film. It is suggested that the film is amorphous. It must be pointed out that the diffraction angles of 22.37° and 25.36° in the

film, which correspond to the silicon substrate because of the pervasion between substrate and the films. Figure 2 presents the AFM image of the film. It can be seen that the film has compact structure, smooth surface, and no crystal grain. Figure 3 shows the transmission spectra of TiO_2 thin film as-deposited on glass substrate. TiO_2 thin film is transparent in the visible range, and the transparency shows a sharp decrease in the UV region owing to the absorption of light[11,12]. Optical transmittance spectrum can be used to derive the energy gap (E_g) of the TiO_2 film. The absorption coefficient, α, can be derived from[13]

$$T = \frac{(1-R)^2 \exp(-\alpha d)}{1 - R^2 \exp(-2\alpha d)}, \tag{2}$$

where T is the optical transmittance, R is the reflectance, and d is the film thickness. At shorter wavelengths, close to the energy gap, the scattering losses are dominated by the fundamental absorption, and the absorption coefficient is given by[11]

$$\alpha = -\frac{\ln T}{d}. \tag{3}$$

Over the optical absorption edge, the indirect-allowed transitions dominate[12]; and above the threshold of fundamental absorption, the following expression can be written[13,14] :

$$(\alpha h\nu)^{1/2} = \alpha_0 (h\nu - E_g), \tag{4}$$

where $h\nu$ is the photon energy, E_g is the energy gap, and α_0 is a constant which does not depend on the photon energy. From the linear part of $(\alpha h\nu)^{1/2} = f(h\nu)$ dependence, the extrapolated energy gap, E_g, can be obtained for α=0. The energy gap is determined by plotting $(\alpha h\nu)^{1/2}$ versus equivalent energy at the wavelength λ, as shown in Fig. 4. This is called "Tauc plot"[15]. As a result, the energy gap of the TiO_2 thin film is 3.02 eV. We can calculate that the threshold absorption wavelength is 411.6 nm for the TiO_2 thin film. Since the high pressure mercury lamp emits visible light of 404.7, 435.8, 546.1, 577.0–579.0 nm, and UV light of 365 nm, we can conclude that the film can absorb the UV light of 365 nm and the visible light of 404.7 nm from irradiation of high pressure mercury lamp.

Figure 5 plots the absorption spectra of de-ionized water and 0.5, 1, 2.5, 5, 10, and 20 ppm methyl orange solutions. From Fig. 5, we can see that absorption spectra of methyl orange solutions with various concentrations show two characteristic peaks at 270 and 464 nm, respectively. In our study, the absorbance of peak at 464 nm is used to evaluate the absorption of methyl orange solutions with various concentrations, as shown in Fig. 6. Further, linear fitting can be done between absorbance and concentration of methyl orange solution. The equation of fitting straight-line can be expressed as

$$Y = 0.06948X + 0.02063, \tag{5}$$

where Y is the absorbance of methyl orange solution at 464 nm, and X is the concentration of methyl orange solution. From Fig. 6, we can see that the absorbance of methyl orange solution is directly proportional to the

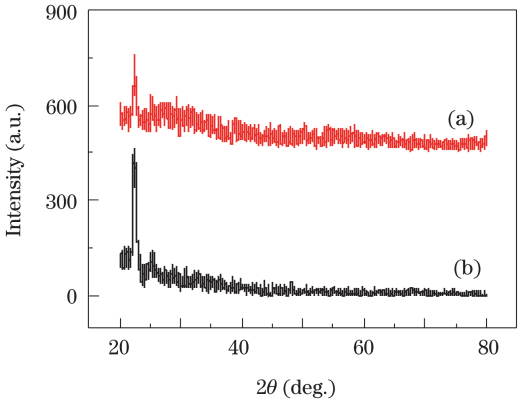

Fig. 1. XRD patterns of (a) as-deposited TiO_2 thin film and (b) silicon substrate.

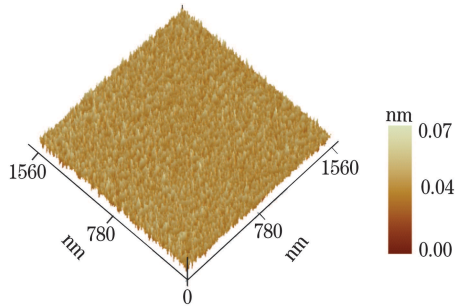

Fig. 2. AFM image of as-deposited TiO_2 thin film.

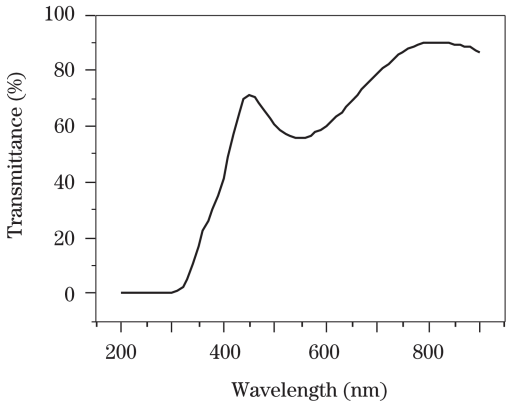

Fig. 3. Transmission spectra of as-deposited TiO_2 thin films.

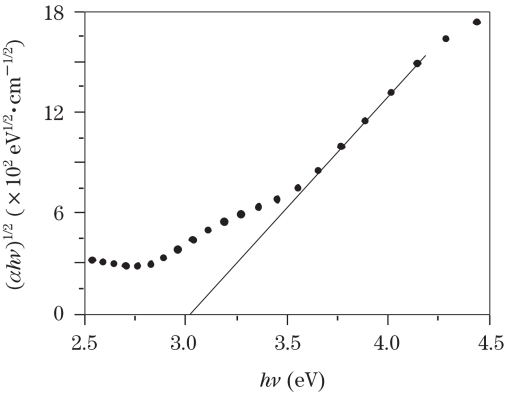

Fig. 4. Determination of energy gap of as-deposited TiO_2 thin films.

concentration. Therefore, after the absorbance of methyl orange solution at 464 nm is obtained, the concentration of methyl orange solution can be calculated from Eq. (5). Figure 7 illustrates the first-order kinetics of photocatalytic degradation of methyl orange solutions of 5, 10, and 20 ppm, as a function of irradiation time over as-deposited TiO_2 thin films. In this figure, A_t is the absorbance of methyl orange after t-min reaction and A_0 is the initial absorbance at 464 nm. From Fig. 7, we can see that $\ln(A_0/A_t)$ is directly proportional to irradiation time.

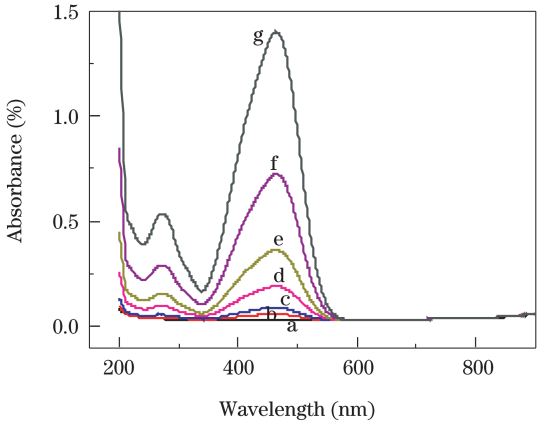

Fig. 5. Absorption spectra of (a) de-ionized water and (b) 0.5, (c) 1, (d) 2.5, (e) 5, (f) 10, and (g) 20 ppm methyl orange solutions.

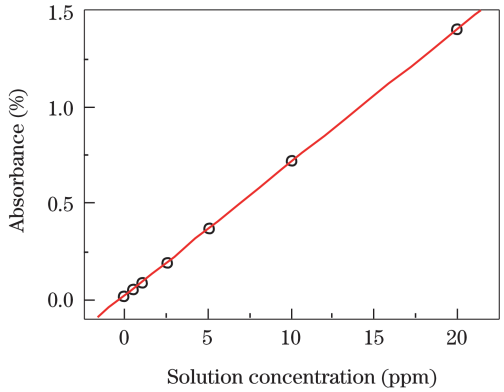

Fig. 6. Dependence of absorbance for 464-nm light on concentration of methyl orange solution.

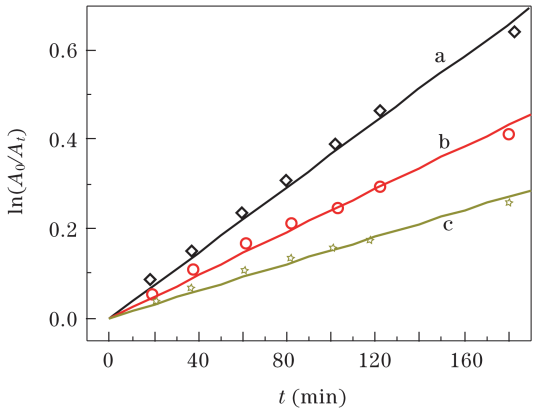

Fig. 7. First-order kinetics of photocatalytic degradation for methyl orange solutions of (a) 5, (b) 10, and (c) 20 ppm concentrations as a function of irradiation time over TiO_2 thin films.

Table 1. Parameters of Photocatalytic Degradation of Methyl Orange Solutions with Different Concentrations by TiO_2 Thin Films

C_0 (ppm)	5	10	20
k (min^{-1})	0.00369	0.0024	0.00151
η (%)	51.246	36.331	25.276

From the above analysis, the absorbance of methyl orange solution is directly proportional to concentration. So we can conclude that the photocatalytic degradation is the first-order reaction and its kinetics can be expressed as

$$ln(C_0/C_t) = kt, \tag{6}$$

where k is the apparent reaction rate constant. The photocatalytic activity can be compared by k value. The k values, which are obtained by linear fitting from Fig. 7, are 0.00369, 0.0024, and 0.00151 for the methyl orange solution concentrations of 5, 10, and 20 ppm, respectively, as shown in Table 1. Based on the absorbance of methyl orange solution at 464 nm, the concentration of methyl orange solution with different initial concentration after 3-h reaction can be calculated from Eq. (5). Furthermore, the degradation rate of methyl orange can be obtained from Eq. (1), as also shown in Table 1. The degradation rate decreases with increasing initial concentration of methyl orange. With the increase of concentration of methyl orange solution, the optical transmission power decreases. So the sum of photon that participating in photocatalysis decreases. Furthermore, as the concentration of methyl orange solution increases, more solute will be adsorbed on the surface of the film, which results in the decrease of active sites, so the degradation rate decreases with the increase of initial concentration.

In conclusion, nano-TiO_2 thin films are deposited on silicon and glass substrates by RF magnetron sputtering using TiO_2 ceramic target. As-deposited TiO_2 thin film is amorphous, and its surface is smooth. The wavelength of the maximum absorbance of methyl orange solution is 464 nm and the absorbance of the solution is directly proportional to its concentration. The photocatalytic degradation of methyl orange solution by the film is the first-order reaction, and the apparent reaction rate constants are 0.00369, 0.0024, and 0.00151 for methyl orange solution concentrations of 5, 10, and 20 ppm, respectively. The degradation rate decreases with the increasing initial concentration of methyl orange.

This work was supported by the National Natural Science Foundation of China (Nos. 50872001 and 50642038), the Scientific Research Foundation of Education Ministry of Anhui Province of China (Nos. KJ2009A006Z, KJ2007B132, and 2005KJ224), the Foundation of Construction of Quality Project of Anhui University of China (No. XJ200907), the Research Foundation for the Doctoral Program of Higher Education of China (No. 20060357003), and the Graduate Student Innovation Programs of Anhui University of China (No. 20072006).

References

1. A. Fujishima and K. Honda, Nature **238,** 37 (1972).
2. C.-H. Li, Y.-H. Hsieh, W.-T. Chiu, C.-C. Liu, and C.-L. Kao, Separ. Purif. Technol. **58,** 148 (2007).
3. J. Yuan, Z. Tang, H. Qi, J. Shao, and Z. Fan, Acta Opt. Sin. (in Chinese) **23,** 984 (2003).
4. P. Gu, H. Chen, M. Ai, Y. Zhang, and X. Liu, Acta Opt. Sin. (in Chinese) **25,** 1005 (2005).
5. Y. Pan, Z. Wu, and L. Hang, Chinese J. Lasers (in Chinese) **35,** 916 (2008).
6. Q. Jia, Y. Le, Y. Tang, and Z. Jiang, Acta Opt. Sin. (in Chinese) **24,** 65 (2004).
7. J. Liu, Z. Wang, A. Li, Q. Hu, and X. Zeng, Chinese J. Lasers (in Chinese) **34,** 765 (2007).
8. M. Wang and Z. Fan, Chinese J. Lasers (in Chinese) **23,** 991 (1996).
9. Q. Ye, P. Y. Liu, Z. F. Tang, and L. Zhai, Vacuum **81,** 627 (2007).
10. J. Zheng, H. Yu, X. Li, and S. Zhang, Appl. Surf. Sci. **254,** 1630 (2008).
11. D. Mardare, G. I. Rusu, F. Iacomi, M. Girtan, and I. Vida-Simiti, Mater. Sci. Eng. B **118,** 187 (2005).
12. D. Mardare, M. Tasca, M. Delibas, and G. I. Rusu, Appl. Surf. Sci. **156,** 200 (2000).
13. H. Tang, K. Prasad, R. Sanjinès, P. E. Schmid, and F. Lévy, J. Appl. Phys. **75,** 2042 (1994).
14. D. Mardare, F. Iacomi, and D. Luca, Thin Solid Films **515,** 6474 (2007).
15. J. Tauc, Mater. Res. Bull. **5,** 721 (1970).